Effect of Bond Thickness on Fracture Behaviour in Adhesive Joints

Cheng Yan[a]; Yiu-Wing Mai[a]; Lin Ye[a]

[a] Department of Mechanical and Mechatronic Engineering J07, Centre of Advanced Materials Technology (CAMT), NSW, Australia

PLEASE SCROLL DOWN FOR ARTICLE

Effect of Bond Thickness on Fracture Behaviour in Adhesive Joints

CHENG YAN, YIU-WING MAI* and LIN YE

Centre of Advanced Materials Technology (CAMT), Department of Mechanical and Mechatronic Engineering J07, The University of Sydney, NSW 2006, Australia

To study the effects of bond thickness on the fracture behaviour of adhesive joints, experimental investigation and finite element analysis have been carried out for compact tension (CT) and double-cantilever-beam (DCB) specimens with different bond thickness. Fractography and fracture toughness exhibited apparent variations with bond thickness. Numerical results indicate that the crack tip stress fields are affected by bond thickness due to the restriction of plastic deformation by the adherends. At the same J level, a higher opening stress was observed in the joint with a smaller bond thickness (h). Beyond the crack tip region, a self-similar stress field can be described by the normalized loading parameter, $J/h\sigma_o$. The relationship between J and crack tip opening displacement, δ, is dependent on the bond thickness. The strong dependence of toughness upon bond thickness is a result of the competition between two different fracture mechanisms. For small bond thickness, toughness is linearly proportional to bond thickness due to the high constraint. After reaching a critical bond thickness, the toughness decreases with further increase of bond thickness due to the rapid opening (blunting) of the crack tip with loading. A simple model has been proposed to predict the variation of toughness with bond thickness.

Keywords: Adhesive joint; Bond thickness; Finite element analysis; Constraint; Fracture mechanism; Fractography; *J*-integral

1. INTRODUCTION

Rubber-toughened epoxies have been widely used to improve the toughness of adhesive joints. An important parameter in adhesive joint design is the bond thickness. Many studies have been conducted

*Corresponding author. Fax: 61-2-9351-7146, e-mail: mai@mech.eng.usyd.edu.au

to investigate the effect of bond thickness on the fracture behaviour of such toughened adhesive joints [1 – 5]. Some investigations showed that that there was an optimum thickness at which a maximum fracture toughness was obtained [1 – 3]. Kinloch and Shaw [4] explained this behaviour in terms of the size of plastic zone imposed by the adherends. A higher toughness is associated with a larger plastic zone. However, Chai [5] showed that the fracture characteristic and energy dissipation mechanisms are not directly related to the size of the crack-tip plastic zone but instead to the fracture surface morphology. Recently, finite element analysis has been performed by Ikeda et al. [6] on edge-crack and tapered double-cantilever-beam (TDCB) adhesive joints. Their results also showed that the area of the plastic zone bears no relationship to the fracture toughness. Further study is, therefore, necessary to unmask the true effect of bond thickness on the fracture behaviour in an adhesive joint.

In this work, the effects of bond thickness on fracture behaviour were investigated experimentally using double-cantilever-beam (DCB) specimens with different bond thickness. Attention was also focused on the elastic – plastic analysis of a crack in compact tension (CT) and double-cantilever-beam (DCB) specimens with different bond thickness (h). The relationship between the J-integral and crack tip opening displacement (CTOD) was investigated. The prediction of the toughness (J_c) variation with bond thickness (h) was also addressed.

2. EXPERIMENTAL PROCEDURE

Experiments were carried out to investigate the effect of bond thickness on the Mode I fracture toughness in a DCB specimen. The adhesive was a diglycidyl ether of bisphenol A (DGEBA) epoxy resin (Araldite® GY 260, supplied by Ciba-Geigy, Australia) modified by 15% liquid rubber (CTBN, 1300X13, BF Goodrich). The curing agent was piperidine. The mechanical properties of the adhesive in tension were measured using tensile specimens [7] and the true-stress and true-strain curve is shown in Figure 1. The elastic properties are: Young's modulus $E = 2.1$ GPa and Possion's ratio $\nu = 0.35$. The adherends were 2024 aluminium and the Young's modulus is $E_s = 71$ GPa and Possion's ratio $\nu_s = 0.3$. Following degreasing with alkaline solution,
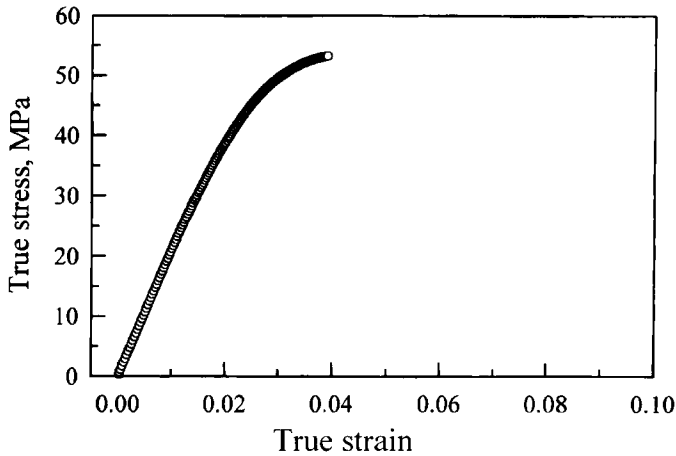
FIGURE 1   True stress–strain relationship for rubber-toughened adhesive.

the bond surfaces were etched in sulfuric acid–sodium dichromate solution (FPL). The bond thickness was chosen as 0.4, 0.6, 0.8, 1.0, 1.5 and 1.8 mm. The dimensions of the DCB specimens are shown in Figure 2(a). The assembled specimens were cured at 120°C for 16 h, followed by slow cooling to ambient temperature. All tests were carried out in an Instron machine at a rate of 1.0 mm/min. The fracture surfaces were observed with a scanning electron microscope (SEM).

3. FINITE ELEMENT MODELLING

Large-deformation finite element analysis was carried out with finite element code ABAQUS (Version 5.7). Plane strain condition was assumed. In addition to the above DCB specimen (referred as DCB(I)), two other specimen geometries were also analyzed. One was the compact tension (CT) geometry with bond thickness of 0.1, 0.4, 1.0, 2.0 and 3.0 mm. Fracture loads for the CT specimens were measured by Fayard *et al.* [8] with exactly the same adhesive as used in this study. Another was the DCB geometry employed by Chai [5], referred to as DCB(II) to differentiate it from DCB(I). The bond thickness was 0.05, 0.1, 0.2, 0.4 and 0.5 mm, respectively. For the
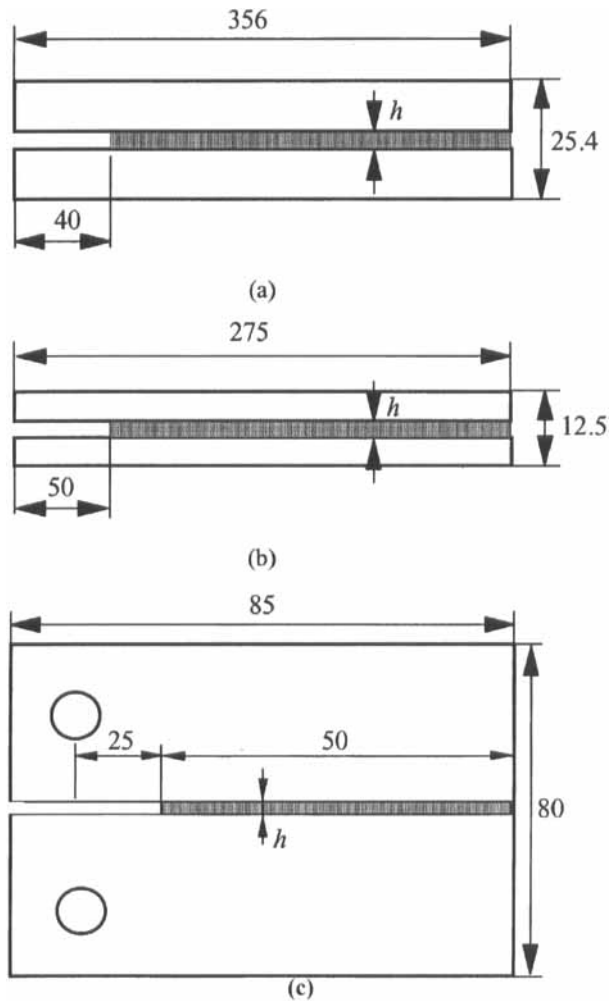
C. YAN *et al.*

FIGURE 2   Adhesive joints: (a) DCB(I), (b) DCB(II) and (c) CT (all dimensions in mm).

DCB(II) specimen, Cycom 907 (BP-907) and aluminium (2024-T3) were chosen as adhesive and adherends, respectively. The mechanical properties and fracture toughness are taken from Chai [5]. The dimensions of the DCB(II) and CT specimens are also shown in Figure 2. Only one-half of the specimen was modelled because of symmetry. The mesh consisted of about $5000 \sim 8000$ elements for the
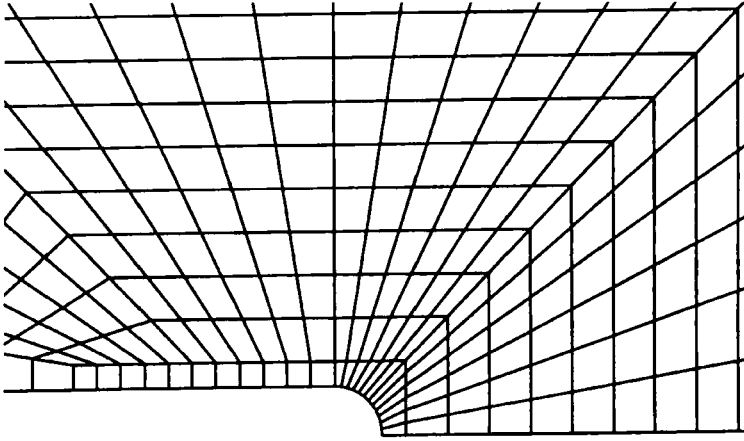
FIGURE 3 Finite element mesh for the crack tip.

specimens. The initial radius of the crack tip was $5\,\mu m$. The details of the mesh at the crack tip are shown in Figure 3. Rate-independent plasticity and associated flow rule were used for the material constitutive model. The J-integral was evaluated according to the domain integral method. The crack-tip opening displacement (CTOD) was measured from the separation between the intercept of two 45°-lines drawn from the crack-tip with the deformed crack profile.

4. RESULTS AND DISCUSSION

4.1. Opening Stress Distribution Ahead of Crack Tip

Figure 4 shows the variation of opening stress (σ_{22}) with loading in the CT specimen ($h = 3$ mm). It can be seen that the opening stress increases with loading (J). A similar trend can be found for other specimens with different bond thickness as well as for the DCB specimens. More recently, the effects of constraint on crack tip stress fields in strength-mismatched welded joints have been studied by Burstow et al. [9] using the finite element method. Their results showed that the opening stress increases with applied loading if the crack is located in the material with lower yield strength (under-matched joint).
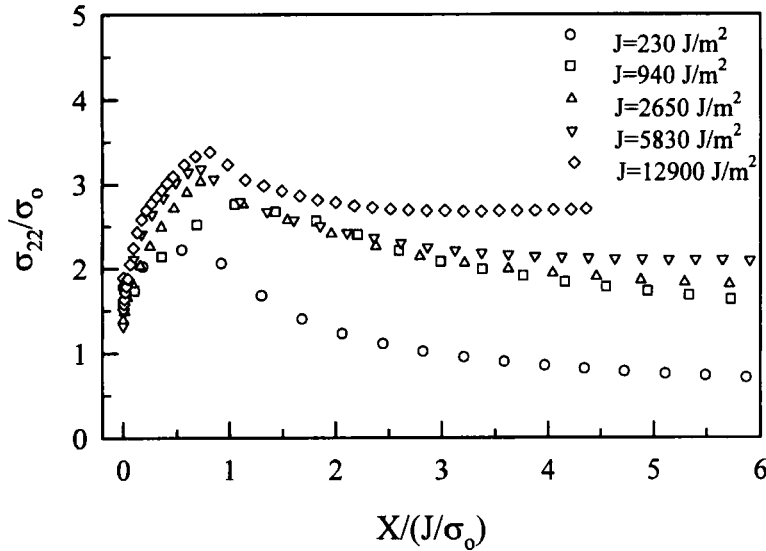
FIGURE 4   Distribution of opening stress (σ_{22}) ahead of crack tip in the CT specimen.

As mentioned in the Introduction, fracture toughness is dependent on the bond thickness for the toughened adhesive joint [1 – 5]. It is, therefore, necessary to compare the stress field ahead of crack tip in the joint with different bond thickness. Figure 5 gives a comparison of the mean stress ($\sigma_m = 1/3(\sigma_{11} + \sigma_{22} + \sigma_{33})$) for the DCB specimens with different bond thickness at the same J. The mean stress is elevated with reduction of bond thickness. In an adhesive joint, the constraint on the crack-tip fields is mainly attributed to the restriction of the plastic zone in the adhesive layer by the adherends. At the same applied load, the plastic zone is more restricted by the adherends for the joint with a smaller bond thickness.

For homogeneous materials in plane strain, the plastic zone size (r_p) can be evaluated approximately by

$$r_p = \frac{1}{6\pi}\left(\frac{K_I}{\sigma_o}\right)^2 = \frac{J}{\sigma_o}\left[\frac{1}{6\pi}\frac{E}{(1-\nu^2)\sigma_o}\right]. \tag{1}$$

It is clear that the size of the plastic zone is approximately scaled by J/σ_o. The relative size of the plastic zone in an adhesive layer with a
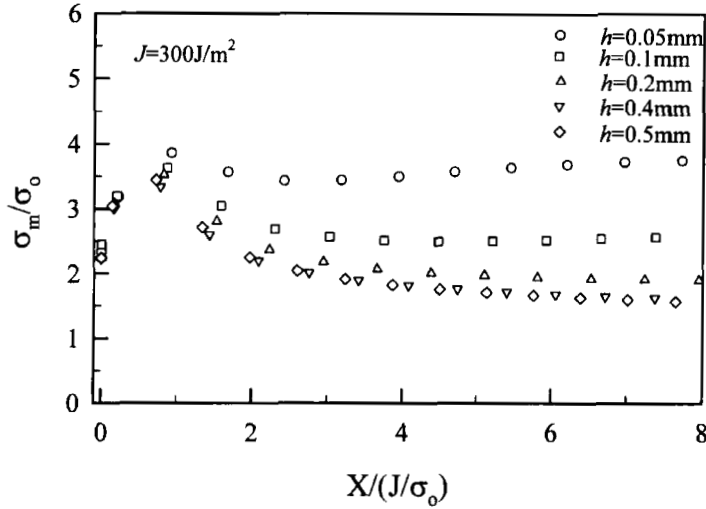
FIGURE 5 Distributions of mean stress (σ_m) in the DCB(II) specimen with different bond thickness.

thickness h is scaled by $J/h\sigma_o$. Therefore, $J/h\sigma_o$ is a potential parameter to indicate the constraint level imposed by the adherends. Figure 6 gives the distributions of opening stress for the CT specimens with
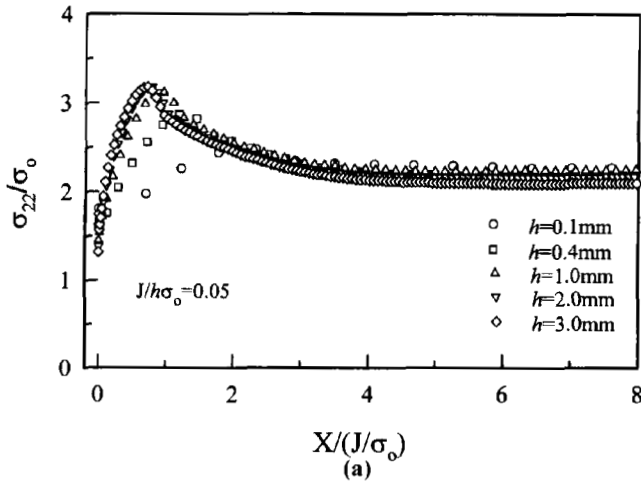

FIGURE 6 Distributions of opening stress (σ_{22}) ahead of crack tip in the CT specimen when parametized by $J/h\sigma_o$: (a) $J/h\sigma_o = 0.05$, and (b) $J/h\sigma_o = 0.1$.
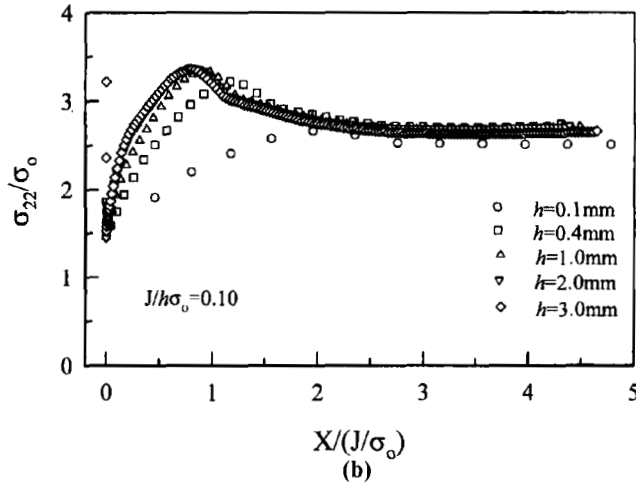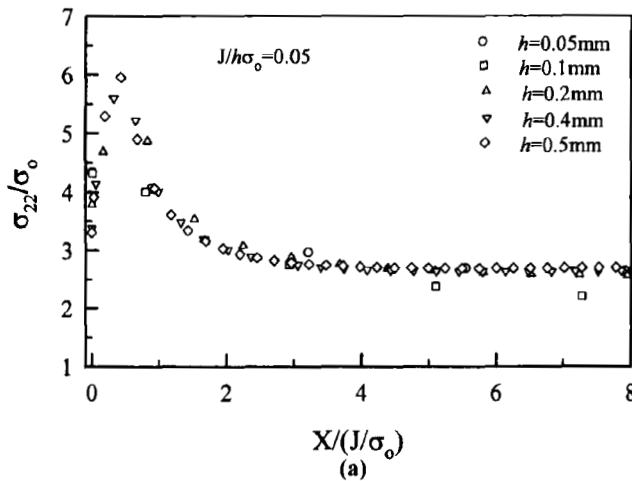
(b)

FIGURE 6   (Continued).

different bond thickness, but loaded to the same value of $J/h\sigma_o$. It can been seen that beyond the crack tip, *i.e.*, $X/(J/\sigma_o) > 2.0$, the stress distributions are similar irrespective of the bond thickness. Figure 7 shows the distributions of opening stress, σ_{22}, for the DCB(II) specimens loaded to the same $J/h\sigma_o$. The same trend can be found for

(a)

FIGURE 7   Distributions of opening stress ahead of crack tip in the DCB(II) specimen when parametized by $J/h\sigma_o$:(a) $J/h\sigma_o = 0.05$, and (b) $J/h\sigma_o = 0.1$.
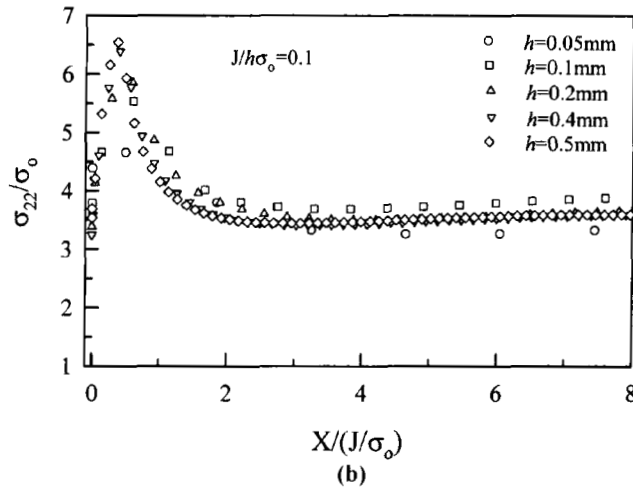
FIGURE 7 (Continued).

the DCB(I) specimens. That is, a similar stress field can be obtained
with the normalised loading parameter, $J/h\sigma_o$. A similar phenomenon
has been observed by Burstow *et al.* [9] for the plastic mis-matched
weld joints.

4.2. Relationship Between *J*-integral and CTOD

In the early work of Shih [10] the relationship between the *J*-integral
and the crack tip opening displacement can be expressed by

$$J = m\sigma_o\delta \tag{2}$$

where δ is the crack tip opening displacement. A large m is associated
with a high constraint condition. Figure 8 shows the variation of m
with the bond thickness, h, in the CT and the DCB(II) specimens.
Clearly, m increases with decreasing bond thickness for both the CT
and the DCB geometry. This is similar to the calculation of Daghyani,
Ye and Mai [11].

4.3. Effect of Bond Thickness on Fracture Toughness

As reviewed in the Introduction, maximum fracture toughness is
usually recorded at a critical bond thickness. For the CT specimen, the
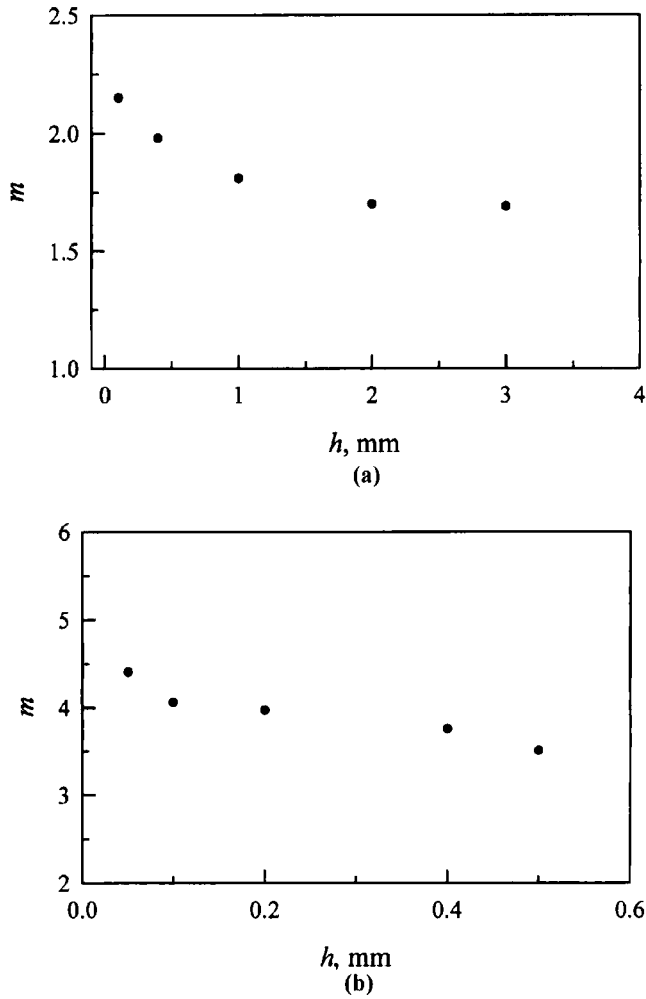
FIGURE 8 Variation of *m* with bond thickness (*h*): (a) CT, and (b) DCB(II) specimens.

fracture loads were measured at different bond thickness [8], as shown in Figure 9(a). The fracture load increased initially then decreased with bond thickness. The maximum fracture load was obtained at 1.00 mm bond thickness. The *J*-integral values corresponding to the fracture loads (J_c) were obtained from the finite element analysis and could be regarded as the fracture toughness. The variation of J_c *versus* bond

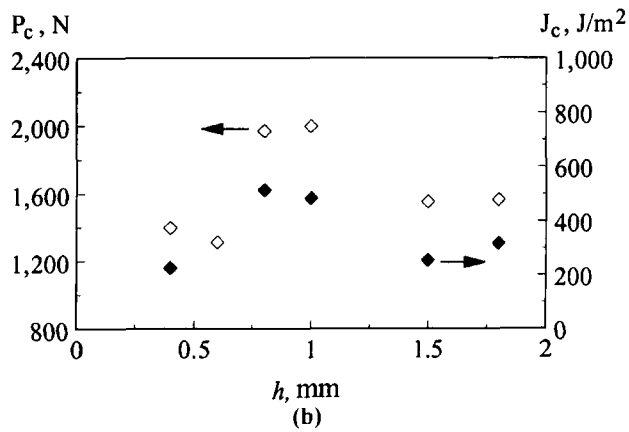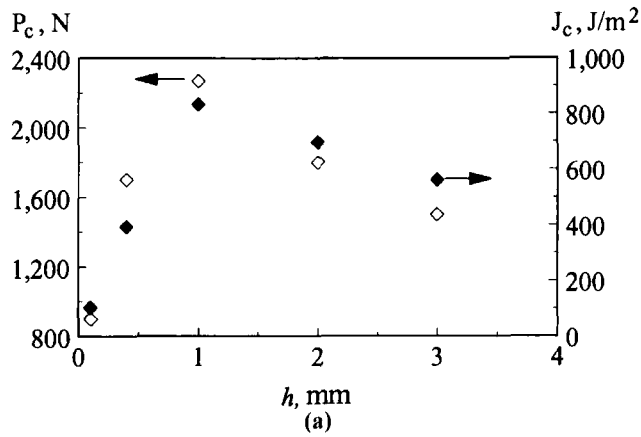FIGURE 9 Fracture load (P_c) and toughness (J_c) at different bond thickness (h) in (a) CT, and (b) DCB(I) specimens.

thickness is also shown in Figure 9(a). As expected, since the fracture loads were used in the FEM calculations, the predicted fracture toughness would mirror the same trend with a maximum J_c at 1.00 mm bond thickness. Also, the J_c corresponding to the measured fracture loads in the DCB(I) specimens were calculated and plotted in Figure 9(b). Similarly, the maximum fracture load and J_c were reached at an intermediate bond thickness of about $0.8 \sim 1.0$ mm. Figure 10 shows the variation of fractographic features with bond

thickness for the DCB(I) specimens. For the thinnest bond ($h =$ 0.4 mm), the fracture surface is flat near the crack initiation site, showing a typical characteristic of brittle fracture. With increasing
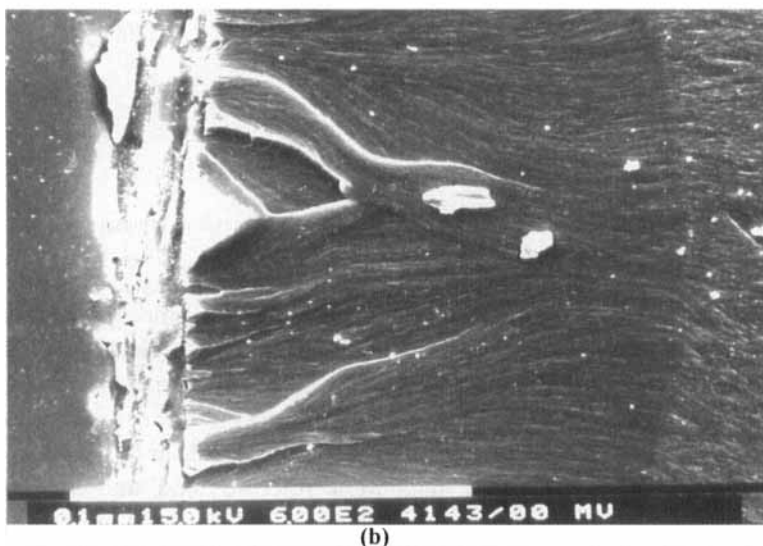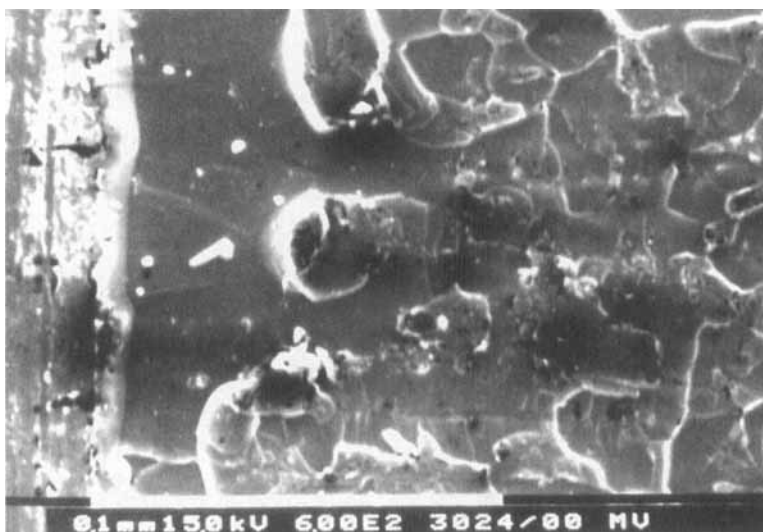

FIGURE 10   Fracture surfaces of DCB(I) specimens: (a) $h = 0.4$ mm, (b) $h = 0.6$ mm, (c) $h = 0.8$ mm, and (d) $h = 1.6$ mm.
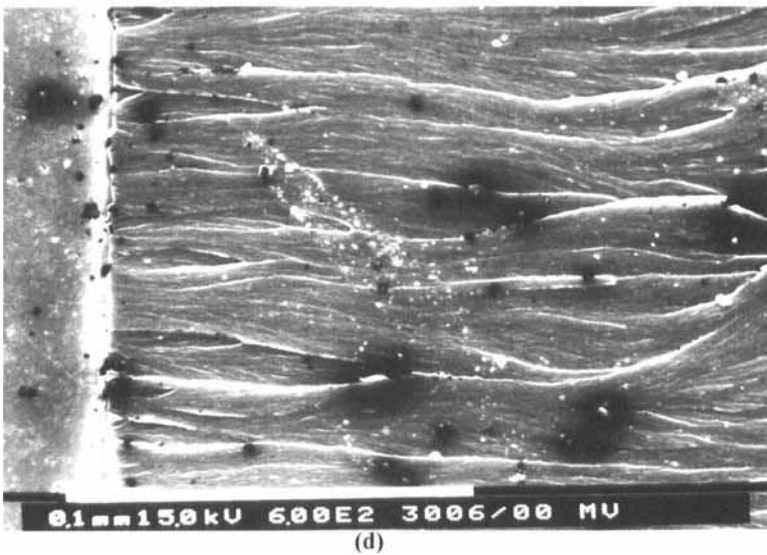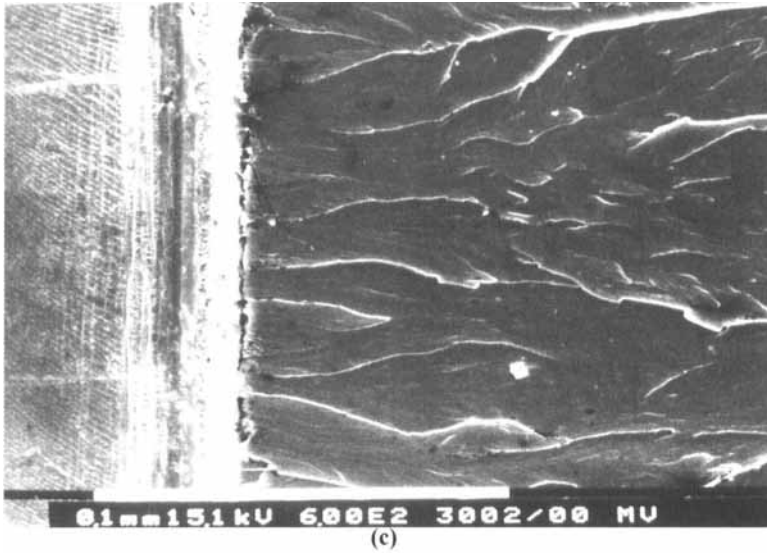
FIGURE 10 (Continued).

bond thickness to 0.6 mm, some "river" marks appear at the pre-crack tip, then followed by a relatively smooth fracture surface. The amount of river marks increases with further increase of bond thickness.

Therefore, it is likely that fracture is controlled by two different fracture mechanisms with a transition at about 0.8 mm. Thick bonds allows more plastic deformation at the crack-tip before fracture initiation. Recently, fractographic features corresponding to different bond thickness was observed by Daghyani et al. [12] using the same material and specimen geometry (CT) as used in this study. They found that a brittle fracture mechanism was associated with thin bonds ($h < 0.5$ mm) but a ductile fracture mechanism was predominant for thick bonds ($h > 1.0$ mm).

The high constraint in thin bonds is expected as the main reason for low toughness. The toughness increases initially with increasing bond thickness due to the relief of constraint, as shown in Figure 9. A very interesting phenomenon is that toughness drops again after further increase of bond thickness. A possible explanation is that increasing bond thickness increases the possibility of incurring internal flows that may trigger failure [5]. Another explanation was given by Bredzs [13], which was that a thick bond prompts necking and lateral deformation in an adhesive joint, resulting in a loss of joint strength.

4.4. Toughness Prediction in Adhesive Joint

Varias et al. [14] showed that two competing fracture mechanisms existed for a constrained ductile layer in rigid adherends. In a very thin layer, cavitation at the site of high triaxial stresses ahead of the crack-tip may precede coalescence. On the other hand, crack tip blunting may result in void-crack coalescence in a thick layer. For an under-matched welded joint, Smith [15] used a critical crack tip opening displacement to evaluate the variation of the J-integral with crack size and weld thickness. Therefore, based on the above observations by these previous investigators and the fractographic observation in Figure 10, it is reasonable to assume that for thin bonds fracture is mainly controlled by a critical opening stress or triaxial stress but a critical crack tip opening displacement is more suitable for joint with a thick bond. In Figures 6 and 7, the opening stress, σ_{22}, is only scaled by the dimensionless parameter, $J/h\sigma_o$. It is widely accepted that brittle fracture is controlled by a critical opening stress. To achieve the critical opening stress, the same $J/h\sigma_o$ must be achieved by the joints

with different bond thickness. Therefore, at the moment of fracture, we have

$$\frac{J}{\sigma_o h} = C_m \tag{3}$$

where C_m is a constant which depends on the magnitude of the critical stress. Then, the fracture toughness (J_c) can be expressed as

$$J_c = C_m \sigma_o h. \tag{4}$$

It is clear in Eq. (4) that the fracture toughness, J_c, is proportional to the bond thickness. C_m can be calibrated from the fracture toughness corresponding to a certain bond thickness (h). Then, this constant can be applied to Eq. (4) to predict the toughness associated with other bond thicknesses. Figure 11(a) gives a comparison between predicted values according to Eq. (4) and J_c values corresponding to the respective bond thicknesses. The agreement is very good for h less than 1 mm, i.e., for thin bonds. With increasing bond thickness, fracture is more likely to be controlled by the critical crack tip opening
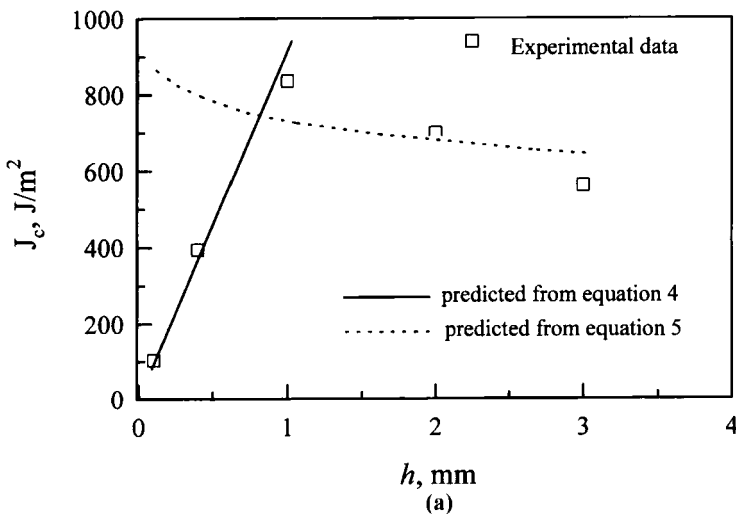

FIGURE 11 Prediction of fracture toughness (J_c) with bond thickness (h): (a) CT, and (b) DCB(I) specimens.
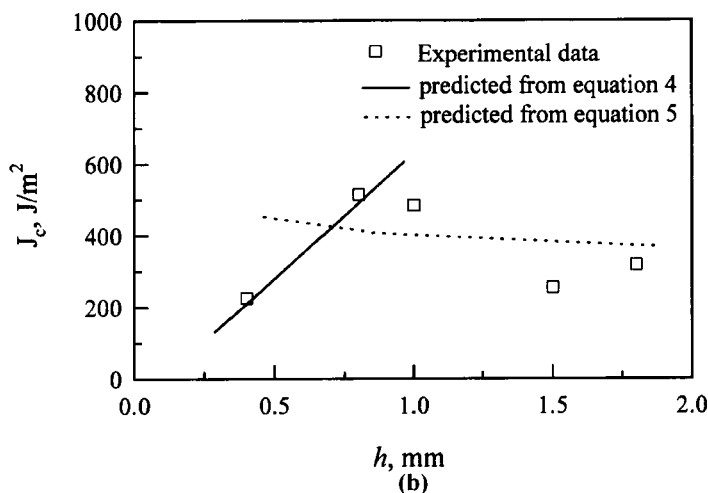
FIGURE 11   (Continued).

displacement (δ_c). By rearranging Eq. (2), we have

$$\delta_c = \frac{J}{m\sigma_o}.$$ (5)

Obviously, fracture toughness depends on both δ_c and m. For a given material, the toughness is controlled by m. In Figure 8, m decreases with increasing bond thickness (h). Thus, to achieve a critical crack tip opening displacement (δ_c) a small J is needed for the joint with a thick bond. In other words, toughness increases with decreasing bond thickness due to the high constraint suppressing the plastic deformation at the crack tip (blunting). This is similar to the explanation given by Bredzs [13]. δ_c can also be calibrated from a joint with a large bond thickness. Then, the variation of fracture toughness, J_c, with bond thickness can be predicted from δ_c and m. As shown in Figure 11(a), the toughness predictions for the CT specimens (dashed line) give the same trend as the calculated J_c when $h > 1$mm For the DCB(I) specimens, the experimental results together with predictions made by Eq. (4) (solid line) and Eq. (5) (dashed line) are shown in Figure 11(b). Clearly, the predictions capture the trend of toughness variation with bond thickness.

Therefore, the variation of toughness in an adhesive joint is likely to be a direct result of the competition between two different fracture mechanisms, *i.e.*, brittle fracture due to high opening stress and ductile fracture by crack tip blunting. For small bond thickness, fracture toughness is linearly proportional to thickness. After reaching a critical bond thickness, fracture toughness decreases with further increase of bond thickness due to the rapid opening (blunting) of the crack tip with applied loading. The critical bond thickness, at which the fracture mechanism changes, is dependent on the specimen geometry and the mechanical properties of both the adhesive and adherends, as shown in Figures 11(a) and 11(b).

For homogeneous materials, the initiation of a ductile tear at a sharp crack was investigated by Wu, Mai and Cotterell [16]. By embedding the growth of an isolated void in a J-Q stress field, the initiation toughness for any geometry and size can be predicted in terms of its value for a standard specimen. To predict initiation toughness in adhesive joints, it is necessary to obtain a better understanding of the variation of the fracture mechanism with bond thickness and specimen geometry. Also, further investigation on the similarity of crack-tip fields in different specimen geometry and size is much needed.

5. CONCLUSIONS

Based on experimental investigation and large deformation finite element analyses for several specimen geometry with different bond thickness, the following conclusions can be drawn:

1. For both CT and DCB specimens with a toughened adhesive, the fracture toughness initially increases with bond thickness then decreases with further increase of bond thickness.
2. The crack-tip stress fields are affected by bond thickness due to the restriction by the adherends. At the same J level, a higher opening stress is observed in the joint with a smaller bond thickness.
3. Beyond the crack-tip region, a self-similar stress field can be described by the normalized loading parameter, $J/h\sigma_o$. The relationship between J and crack tip opening displacement, δ, is dependent on the bond thickness.

4. Fractographic observations confirm that the failure mechanisms also vary with the bond thickness. The strong dependence of toughness upon bond thickness is the result of the competition between two different fracture mechanisms. For small bond thickness, toughness is linearly proportional to bond thickness due to the high constraint imposed. After reaching a critical bond thickness, the toughness decreases with further increase of bond thickness due to the rapid opening (blunting) of the crack tip with loading. A simple model has been proposed to predict the variation of toughness with bond thickness and there is good agreement with experimental data.

Acknowledgments

References

[1] Bascom, W. D., Cottington, R. L., Jones, R. L. and Peyser, P., *J. App. Polym. Sci.* **19**, 2545–2562 (1975).
[2] Bascom, W. D. and Cottington, R. L., *J. Adhesion* **7**, 333–346 (1976).
[3] Hunston, D. J., Kinloch, A. J. and Wang, S. S., *J. Adhesion* **28**, 103–114 (1989).
[4] Kinloch, A. J. and Shaw, S. J., *J. Adhesion* **12**, 59–77 (1981).
[5] Chai, H., In: *Composite Materials: Testing and Design, ASTM STP 893* Whitney, J. M. Ed. (ASTM, Philadelphia, 1986), pp. 209–231.
[6] Ikeda, T., Miyazaki, N., Yamashita, A. and Munakata, T., In: *Composites for the Pressure Vessel Industry, ASME, PVP-Vol. 302* Bees, W. J. *et al.* Eds., pp. 155–162 (1995).
[7] Xiao, K. Q. and Ye, L., Private communication (1998).
[8] Fayard, N. and Ye, L., Private communication (1998).
[9] Burstow, M. C., Howard, I. C. and Ainsworth, R. A., *J. Mech. and Phys. of Solids* **46**, 845–872 (1998).
[10] Shih, C. F., *J. Mech. and Phys. of Solids* **29**, 305–326 (1981).
[11] Daghyani, H. R., Ye, L. and Mai, Y. W., *J. Adhesion* **53**, 163–172 (1995).
[12] Daghyani, H. R., Ye, L. and Mai, Y. W., *J. Adhesion* **53**, 149–162 (1995).
[13] Bredzs, N., *Welding Journal* **33**, 545-s (1954).
[14] Varias, A. G., Suo, Z. and Shih, C. F., *J. Mech. Phys. Solids* **39**, 963–986 (1991).
[15] Smith, E., *Internat. J. Fracture* **53**, 33–42 (1992).
[16] Wu, S. X., Mai, Y. W. and Cotterell, B., *J. Mech. Phys. Solids* **43**, 793–810 (1995).